Received: 24 February 2022 | Revised: 27 July 2022 | Accepted: 27 July 2022

DOI: 10.1111/jon.13035

JOURNAL OF NEUROIMAGING
THE OFFICIAL JOURNAL OF THE AMERICAN SOCIETY OF NEUROIMAGING
WILEY

CLINICAL INVESTIGATIVE STUDY

Comparison of axial and sagittal spinal cord motion measurements in degenerative cervical myelopathy

Nikolai Pfender[1] | Jan Rosner[1,2] | Carl Moritz Zipser[1] | Susanne Friedl[1] | Kevin Vallotton[1] | Reto Sutter[3] | Markus Klarhoefer[4] | Martin Schubert[1] | Michael Betz[5] | José Miguel Spirig[5] | Maryam Seif[1,6] | Michèle Hubli[1] | Patrick Freund[1] | Mazda Farshad[5] | Armin Curt[1,5] | Markus Hupp[1]

[1]Spinal Cord Injury Center, Balgrist University Hospital, University of Zurich, Zurich, Switzerland

[2]Department of Neurology, Bern University Hospital, Inselspital, University of Bern, Bern, Switzerland

[3]Radiology, Balgrist University Hospital, University of Zurich, Zurich, Switzerland

[4]Siemens Healthcare AG, Zürich, Switzerland

[5]University Spine Centre Zurich, Balgrist University Hospital, University of Zurich, Zurich, Switzerland

[6]Department of Neurophysics, Max Planck Institute for Human Cognitive and Brain Sciences, Leipzig, Germany

Correspondence
Markus Hupp, Spinal Cord Injury Center, Balgrist University Hospital, University of Zurich, Forchstr. 340, 8008 Zurich, Switzerland.
Email: Markus.Hupp@balgrist.ch

Funding information
Balgrist Stiftung, Zurich, Switzerland; SNF Eccellenza Professorial Fellowship, Grant/Award Number: PCEFP3_181362/1; Wings for Life, Grant/Award Number: WFL-CH-19/20

Abstract

Background and Purpose: The timing of decision-making for a surgical intervention in patients with mild degenerative cervical myelopathy (DCM) is challenging. Spinal cord motion phase contrast MRI (PC-MRI) measurements can reveal the extent of dynamic mechanical strain on the spinal cord to potentially identify high-risk patients. This study aims to determine the comparability of axial and sagittal PC-MRI measurements of spinal cord motion with the prospect of improving the clinical workup.

Methods: Sixty-four DCM patients underwent a PC-MRI scan assessing spinal cord motion. The agreement of axial and sagittal measurements was determined by means of intraclass correlation coefficients (ICCs) and Bland-Altman analyses.

Results: The comparability of axial and sagittal PC-MRI measurements was good to excellent at all cervical levels (ICCs motion amplitude: .810-.940; $p < .001$). Significant differences between axial and sagittal amplitude values could be found at segments C3 and C4, while its magnitude was low (C3: 0.07 ± 0.19 cm/second; C4: −0.12 ± 0.30 cm/second). Bland-Altman analysis showed a good agreement between axial and sagittal PC-MRI scans (coefficients of repeatability: minimum −0.23 cm/second at C2; maximum −0.58 cm/second at C4). Subgroup analysis regarding anatomic conditions (stenotic vs. nonstenotic segments) and different velocity encoding (2 vs. 3 cm/second) showed comparable results.

Conclusions: This study demonstrates good comparability between axial and sagittal spinal cord motion measurements in DCM patients. To this end, axial and sagittal PC-MRI are both accurate and sensitive in detecting pathologic cord motion. Therefore, such measures could identify high-risk patients and improve clinical decision-making (ie, timing of decompression).

KEYWORDS
cervical stenosis, degenerative cervical myelopathy, phase contrast MRI, spinal cord compression, spinal cord oscillation, spinal cord motion

INTRODUCTION

Degenerative changes of the cervical spine may result in cervical spinal stenosis with consecutive spinal cord compression leading to the clinical imprint of degenerative cervical myelopathy (DCM). DCM is the most common cause of nontraumatic incomplete spinal cord injury.[1,2] While standard of care is decompressive surgery in DCM patients with moderate and severe impairments, treatment decisions (operative vs. conservative) in mild DCM are still challenging.[3] The clinical assessments such as modified Japanese Orthopaedic Association (mJOA) score are good ad hoc measures but are rather insensitive to reveal deterioration at an early stage of DCM and to identify patients at risk.[4] The pathophysiology of DCM is attributed to immediate (ie, direct or static) cord compression, spinal malalignment leading to altered cord tension, impaired vascular supply, and repeated dynamic injury.[5–8] Dynamic spinal cord injury is often narrowed to segmental hypermobility; however, cardiac-related periodic cord motion may play a by far underestimated role in this pathophysiological consideration. The cervical spinal cord is subject to a physiological craniocaudal motion supposedly due to cardiac pulse wave dynamics, which can be assessed by phase contrast MRI (PC-MRI).[9,10] Previous studies, applying 2-dimensional PC-MRI, demonstrated increased spinal cord motion at the level of a cervical spinal stenosis.[11–15] Interestingly, increased motion was associated with sensorimotor deficits[12,14] and impaired electrophysiological readouts.[14,15] Thus, altered spinal cord motion may be a potential biomarker of spinal cord dysfunction, identifying patients at risk for disease progression. However, to date no standardized PC-MRI protocol has been established (plethora of readouts of spinal cord motion[12,14–17]; axial[9–11,15,18] and sagittal PC-MRI[12,16,17,19]). Recently, sagittal phase contrast measurements[16,17] and the axial imaging[9,11] were reported to assess craniocaudal spinal cord motion. However, the agreement between these two approaches remains unclear. While axial measurements are adapted to the alignment of the spinal cord (slice orientation perpendicular to the spinal cord; Figure 1A), sagittal measurements may be confounded by a misalignment of the spinal cord in the sagittal field of view, causing a systematic measurement error.

This study therefore aims to determine the agreement of axial and sagittal PC-MRI measurements of spinal cord motion with the prospect of improving the clinical workup of DCM patients. We hypothesized that sagittal spinal cord motion measurements may be confounded by the misalignment of the spinal cord within the field of view and can therefore not be as accurate as axial measurements that are aligned perpendicular to the spinal cord.

METHODS

Study design and population

This prospective, cross-sectional, single-center study recruited 64 DCM patients from the outpatient clinic of the University Spine Center, University Hospital Balgrist, Zurich between March 2019 and August 2021. Inclusion criteria were as follows: a cervical spinal stenosis on T2-weighted (T2w) MRI; clinical symptoms consistent with DCM (ie, pain, sensory, or motor deterioration in the upper or lower limbs, gait, or bladder dysfunction); no other neurological disorder (identified by medical history and neurological examination); age 18-80 years; and no MRI contraindications. Symptom severity and functional impairment were assessed with the mJOA score[20] and complementary clinical examinations (ie, a thorough standardized neurological examination according to the International Standards for Neurological Classification of Spinal Cord Injury including segmental sensory assessments and motor scores[21]; the Graded and Redefined Assessment of Strength and Prehension for hand function[22]). DCM was diagnosed in patients with at least one clinical symptom and sign of cervical myelopathy[23] complemented by corresponding stenosis in cervical spine MRI. Some patients in our population were rated with an mJOA score of 18, while symptoms consistent with DCM were observed in the complementary assessments.

Standard protocol approvals, registrations, and patient consents

This prospective study was approved by the local ethics committee (Kantonale Ethikkommission Zurich, KEK-ZH 2012-0343, BASEC Nr. PB_2016-00623) and registered (www.clinicaltrials.gov; NCT 02170155). The work described has been carried out in accordance with The Code of Ethics of the World Medical Association (Declaration of Helsinki) for experiments involving humans. Informed consent was obtained from all participants prior to study enrolment. Study data were collected and managed using REDCap electronic data capture tools hosted at Balgrist University Hospital, Zurich, Switzerland.[24]

Imaging

The MRI setup was supported by a radiologist (RS) and a physicist (MK). All subjects underwent a 3T MRI scan (MAGNETOM Prisma; Siemens Healthcare GmbH, Erlangen, Germany) including sagittal T2w and axial

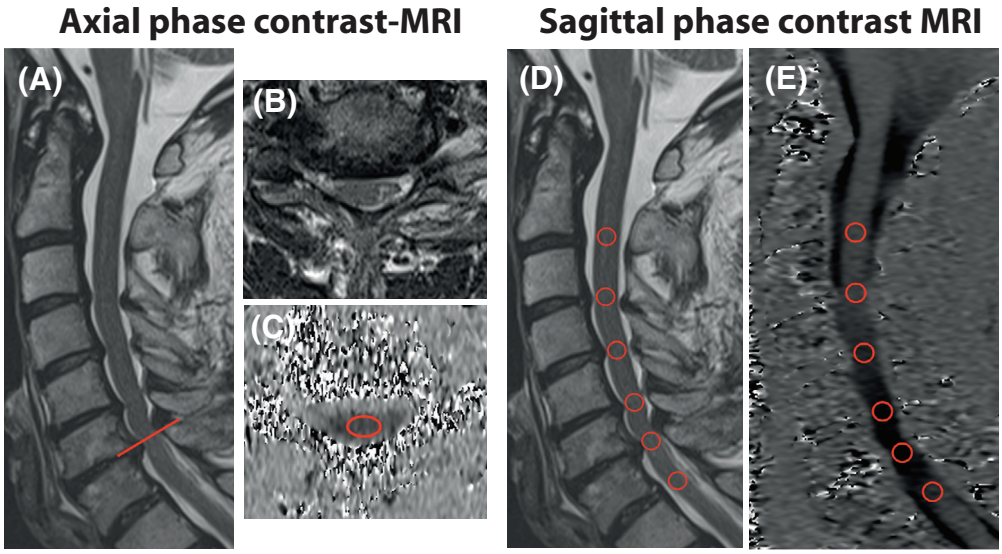

FIGURE 1 Illustrative example of axial and sagittal phase contrast measurements. In a patient with a multisegmental cervical stenosis, maximum stenosis was observed at segment C6 (A; midsagittal T2 weighted [w]; B; axial T2w). Spinal cord motion was assessed with an axial phase contrast-MRI (PC-MRI) slice (C), orientated perpendicular to the spinal cord (A; red line showing slice orientation) with a predefined region of interest (ROI) (C; axial PC-MRI; segment C6; ROI = red ellipse). In sagittal phase contrast imaging, all cervical segments were obtained with a predefined ROI (D; midsagittal T2w; E; midsagittal PC-MRI; ROIs = red circles). Velocity in PC-MRI (C, axial PC-MRI; E, sagittal PC-MRI) was encoded in gray values, while darker colors represent higher caudal motion.

TABLE 1 Parameters of MRI sequences

	Axial T2w	Sagittal T2w	Axial PC	Sagittal PC
TE (ms)	93	87	12.36	12.36
TR (ms)	3600	3760	60.84	60.28
Slice thickness (mm)	3	2.5	5	5
Flip angle (°)	90/150	90/160	10	10
Field of view (mm)	160	220	140	180
Bandwidth (Hz/px)	284	260	355	355
Base resolution	320	384	256	256
Phase resolution	80%	75%	50%	50%
Spatial resolution (mm^3)	0.5 × 0.6 × 3.0	0.6 × 0.8 × 2.5	0.3 × 0.6 × 5.0	0.4 × 0.8 × 5.0
Parallel imaging technique	GRAPPA 2	None	None	None

Abbreviations: GRAPPA, GeneRalized Autocalibrating Partial Parallel Acquisition; TE, echo time; TR, repetition time; w, weighted.

T2w MRI. Spinal cord motion was assessed with sagittal and axial PC-MRI retrospectively cardiac gated using a finger clip (MRI parameters are listed in Table 1). The 2-dimensional phase contrast sequence encoded craniocaudal spinal cord motion. The velocity encoding (venc) value was set to 2 or 3 cm/second (from April 2020) based on previous findings of cord motion.[9,12–15,18] Velocity signal was assessed within 20 time points during a cardiac cycle and 128 cardiac cycles were acquired per measurement. Slice orientation in axial PC-MRI (measurement at the corresponding intervertebral disc level) was adjusted perpendicular to the spinal cord (Figure 1A); sagittal phase contrast measurements were placed midsagittal into the spinal cord (Figure 1D). While in sagittal PC-MRI no adaption to the alignment of the spinal cord is possible for each individual cervical segment, it may be confounded by the misalignment of the cord to the vertical reference line within the field of view (Figure 2), which may cause a systematic measurement error. Total acquisition time was approximately 23 minutes.

Cervical segments were classified as "stenotic" or "nonstenotic." A stenotic segment was defined as a loss of the cerebrospinal fluid (CSF) signal in axial T2w imaging ventral and dorsal to the spinal cord. Segments with visible CSF signal in axial T2w imaging ventral and/or dorsal to the spinal cord were defined as nonstenotic. In axial PC-MRI in patients with a monosegmental stenosis, the C2 segment and the stenotic segment were measured. In patients with a multisegmental stenosis, the C2 segment and the most stenotic segment (defined

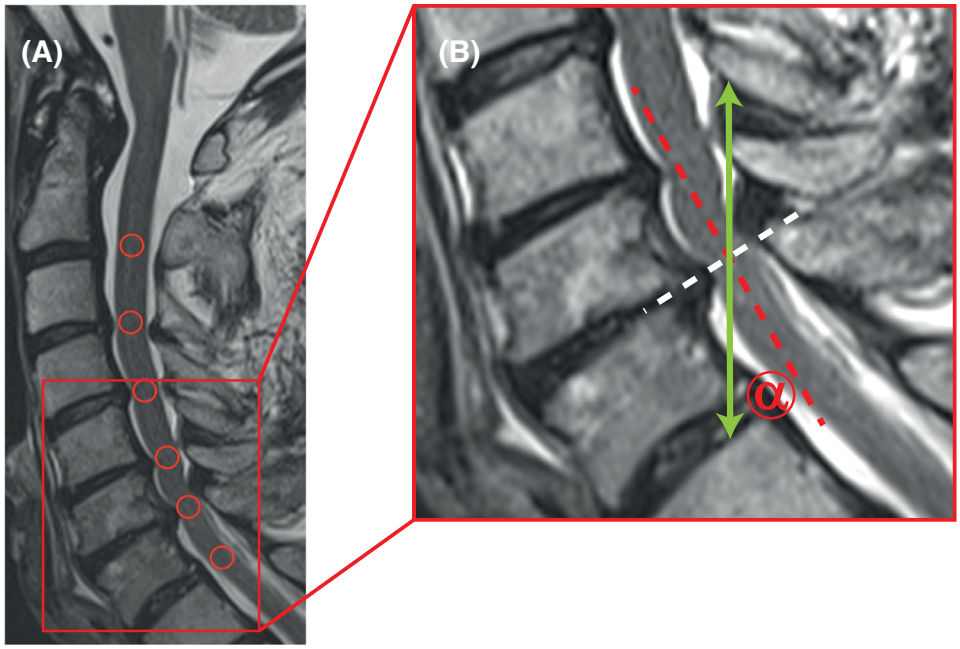

FIGURE 2 Misalignment of the spinal cord in sagittal phase contrast MRI. In a patient with a multisegmental cervical spinal stenosis, the spinal cord shows a lordotic flection (A; midsagittal T2 weighted [w]; red circles representing phase contrast MRI [PC-MRI] regions of interest). In axial imaging, the slice orientation was adjusted perpendicular to the spinal cord (B; midsagittal T2w, magnification of the red section in panel A, white dotted line representing the orientation of the axial PC-MRI slice), measuring appropriately through plane craniocaudal spinal cord motion. In contrast, in sagittal PC-MRI spinal cord motion was assessed craniocaudal within the field of view (B; midsagittal T2w; magnification of the red section in panel A; green arrow represents the orientation of the craniocaudal PC-MRI velocity measurements), while the spinal cord was misaligned to the vertical reference line (B; sagittal T2w; magnification of the red section in panel A; dotted red line representing the spinal cord orientation at the level of the cervical disc C6/C7). The misalignment (B; sagittal T2w; magnification of the red section in panel A; misalignment angle α) may confound craniocaudal spinal cord motion measurements by a systematic measurement error.

as maximum spinal canal narrowing) were measured. The stenotic respectively the most stenotic segment was judged visually in T2w imaging by two investigators (NP, MH; consultant neurologists). In all patients, additional axial PC-MRI measurements at as many as possible other stenotic (multisegmental stenosis) and nonstenotic (monosegmental and multisegmental stenosis) cervical segments were obtained. In sagittal PC-MRI, all cervical segments were measured.

Imaging analysis

Image processing was performed using the Horos free DICOM viewer (www.horosproject.org) by two experienced investigators (NP, MH; consultant neurologists). Phase contrast images were visually controlled for artifacts prior to image processing. In axial phase contrast measurements, craniocaudal spinal cord motion was determined by a predefined ellipsoid-shaped region of interest (30.56 mm^2) midcentered into the spinal cord (Figure 1C). In sagittal measurements, a predefined round-shaped region of interest (20.03 mm^2) was centered on the spinal cord at the corresponding cervical intervertebral disc level (Figure 1E). Velocity calculation was conducted as reported previously.[9,11] PC-MRI spinal cord motion readouts included the amplitude (maximum negative peak to maximum positive peak) of the velocity signal over the cardiac cycle. The misalignment angle α was measured between the spinal cord orientation at the segmental cervical disc level (perpendicular to the axial PC-MRI slice; red dotted line; Figure 2) and the vertical reference line (orientation of the craniocaudal velocity measurement; green arrow; Figure 2) within the field of view.

Statistical analysis

Statistical analysis was conducted using SPSS (IBM SPSS Statistics for Windows, Version 26.0. Armonk, NY; IBM Corp). Metrics are reported as group mean ± standard deviation (SD). Statistical significance was set at <.05. Spinal cord motion values were compared in each cervical segment (C2 = segment C2/C3; C3 = segment C3/C4; C4 = segment C4/C5; C5 = segment C5/C6; C6 = segment C6/C7) separately, as previous work showed significant differences of spinal cord motion between the cervical segments.[9,16] At segment C7/T1, no comparison of axial and sagittal PC-MRI was possible as no axial measurement was available.

Statistical analyses were conducted in the whole group (all collected measurements); additional subgroup analysis was performed with regard to the velocity encoding (2 vs. 3 cm/second) and in stenotic and nonstenotic segments separately. All data were tested for normal distribution by means of histograms and Shapiro-Wilk test. If

differences of axial minus sagittal spinal cord motion values were normally distributed (all measurements: amplitudes C4, C5, and C6; subgroup venc 2 cm/second: amplitudes C4, C5, and C6; subgroup venc 3 cm/second: amplitudes C2, C3, C5, and C6; subgroup nonstenotic segments: amplitudes C3 and C5; subgroup stenotic segments: amplitudes C4, C5, and C6), a one-sample *t*-test was used to test if the mean differences of the amplitude values between the two methods (ie, axial minus sagittal PC-MRI value) were significantly different from zero. In not normally distributed data, a one-sample Wilcoxon test was used. If the mean or median difference of a parameter was different from zero, there was no agreement between axial and sagittal PC-MRI measurements. Comparability of axial and sagittal PC-MRI was examined by intraclass correlation coefficients (ICCs; single measures, two-way mixed effects model, absolute agreement) and Bland-Altman analysis[25] to estimate limits of agreement between the two (ie, axial vs. sagittal PC-MRI) methods. The ICC values were characterized as follows: "poor" for <.50, "moderate" for .50-.74, "good" for .75-.90, and "excellent" for >.90.[26] Between subgroup differences were evaluated with the Mann-Whitney *U* test (amplitude differences; amplitude values; age; misalignment angle of the spinal cord) and Fishert's exact test (number of stenotic segments; proportion of measurements in stenotic segments; site of the maximum spinal cord compression; sex). Correlations between the amplitude differences and the misalignment angle α and between the amplitude difference and the corresponding amplitude mean value were tested by calculation of Spearman-Rho coefficients.

Data availability

The MRI data acquired and processed in the present study are available from the corresponding author upon request with the need for a formal data sharing agreement.

RESULTS

Patient demographics

Sixty-four patients (40 (62.5%) male; age: 56.6 ± 14.7 years) were enrolled (Table 1). Twenty-three patients (35.9%) presented with a single stenosis, and 41 (64.1%) had multiple stenotic segments (number of stenotic segments: 2.05 ± 1.02). mJOA score ranged from 11 to 18 (15.70 ± 2.14). Twenty-five (39.1%) patients showed hyperintensity on T2w MRI consistent with myelopathy. In 64 patients with available sagittal phase contrast imaging (320 segmental measurements in segments C2-C6), a total of 270 segmental axial PC-MRI measurements were performed (Table 2). Five axial (1.9%) and 18 sagittal (5.6%) segmental PC-MRI measurements were excluded from analysis due to artifacts (Table 2). Artifacts in PC-MRI could be attributed to aliasing due to low velocity encoding in axial and sagittal measurements, to infolding artifacts of the shoulders in caudal cervical segments in axial measurements, and to unproper slice placement and motion artifacts (2 patients = 12 segmental datasets) in sagittal measurements. In total, 62 values of axial and sagittal measurements could be compared at segment C2, 43 at C3, 51 at C4, 54 at C5, and 41 at C6.

Spinal cord misalignment in sagittal PC-MRI

Misalignment of the spinal cord to the vertical reference within the field of view in sagittal MRI (Figure 2), potentially causing a systematic measurement error, was most prominent at C6 (13.24 ± 8.27°), but less at segments C2 (6.43 ± 4.53°), C3 (7.32 ± 4.47°), C4 (8.26 ± 6.07°), and C5 (8.53 ± 7.10°). No correlations could be found between the amplitude differences and the misalignment angles in any segment ($p > .169$).

Differences of spinal cord motion values between axial and sagittal measurements

Segmental axial and sagittal amplitude values are illustrated in Table 3 (group mean) and Figure 3 (all measurements; individual values). Over all measurements (venc 2 and 3 cm/second; stenotic and nonstenotic segments), the test of the median or mean differences of the amplitude values (axial minus sagittal PC-MRI values) showed significant differences to zero at the cervical segments C3 (0.07 ± 0.19 cm/second; $p = .001$) and C4 (−0.12 ± 0.30 cm/second; $p = .008$; Table 3).

While results in the whole patient group may be confounded by different measurement techniques (ie, different venc used for measurements) and anatomic conditions (ie, measurements in stenotic vs. nonstenotic segments), subgroup analyses were conducted.

In a subgroup analysis with regard to the different venc used for the measurements, no significant amplitude differences could be found in measurements with venc 2 cm/second ($p > .165$; Table 4). In venc 3 cm/second measurements, amplitude differences were significantly different from 0 in segments C3 (0.07 ± 0.11 cm/second; $p = .001$) and C4 (−0.24 ± 0.25 cm/second; $p < .001$; Table 4).

Additionally, amplitude differences at the C4 level in the subgroup with venc 3 cm/second measurements were higher compared to the subgroup with venc 2 cm/second ($p < .001$), while no significant disagreement could be observed between subgroups in other segments (C2: $p = .832$; C3: $p = .600$; C5: $p = .481$; C6: $p = .754$). There was no significant difference at the C4 level between subgroups with venc 2 cm/second and venc 3 cm/second measurements in terms of age (52.2 ± 17.8 vs. 57.1 ± 12.4 years; $p = .354$), sex (36.8% vs. 40.6% female; $p = 1.000$), the proportion of measurements in stenotic segments (68.4% vs. 50.0%; $p = .250$), the number of stenotic segments within the patient (2.3 ± 1.0 vs. 2.0 ± 1.0; $p = .830$), the misalignment angle of the spinal cord (10.0 ± 6.7° vs. 7.2 ± 5.5°; $p = .071$), and the site of the maximum spinal cord compression (venc 2 cm/second:

TABLE 2 Basic demographics and number of phase contrast measurements

Basic demographics (*N* = 64)	
Sex (male)	40 (62.5%)
Age (years)	56.6 ± 14.7
Monosegmental stenosis	23 (35.9%)
Multisegmental stenosis	41 (64.1%)
Number of stenotic segments	2.05 ± 1.02
mJOA	15.70 ± 2.14
T2w myelopathy	25 (39.1%)

Number of phase contrast measurements

Axial segment	***N***	**Stenotic segment**	**Nonstenotic segment**
C2	64	0	64
C3	44	20	24
C4	57	32 (1)	25 (1)
C5	60	50 (2)	10
C6	45	21	24 (1)
Sagittal segment	***N***	**Stenotic segment**	**Nonstenotic segment**
C2	64	0	64 (2)
C3	64	20 (1)	44 (1)
C4	64	31 (3)	33 (2)
C5	64	51 (2)	13 (3)
C6	64	23 (1)	41 (3)

Number of phase contrast measurements with regard to venc

	venc 2		**venc 3**	
Axial segment	**Stenotic segment**	**Nonstenotic segment**	**Stenotic segment**	**Nonstenotic segment**
C2	0	29	0	35
C3	10	0	10	24
C4	14 (1)	8 (1)	18	17
C5	23 (2)	2	27	8
C6	8	2	13	22 (1)
	venc 2		**venc 3**	
Sagittal segment	**Stenotic segment**	**Nonstenotic segment**	**Stenotic segment**	**Nonstenotic segment**
C2	0	29 (1)	0	35 (1)
C3	10	19 (1)	10 (1)	25
C4	15 (1)	14 (1)	18 (2)	17 (1)
C5	24 (2)	5	27	8 (3)
C6	10	19 (1)	13 (1)	22 (2)

Note: Inside parenthesis is the number of measurements with artifacts.
Abbreviations: mJOA, modified Japanese Orthopaedic Association; *N*, number; venc, velocity encoding; w, weighted.

C3, 21.1%; C4, 31.6%; C5, 47.4%; C6, 0.0% vs. venc 3 cm/second: C3, 15.6%; C4, 18.8%; C5, 50.0%; C6, 15.6%; $p = .292$), but for amplitude values in axial measurements (Table 4; $p = .031$).

In nonstenotic segments, a significant difference from 0 was found for the amplitude differences at segments C3 (0.06 ± 0.10 cm/second; $p = .010$) and C4 (−0.14 ± 0.27 cm/second; $p \leq .010$), while this could be observed in stenotic segments for the amplitude at C3 only (0.10 ± 0.27 cm/second; $p = .049$; Table 5). Additionally, amplitude differences between measurements in stenotic and nonstenotic segments did not show a significant disagreement at any cervical segment (C2: no stenotic segments; C3: $p = .732$; C4: $p = .287$; C5: $p = .389$; C6: $p = .130$).

TABLE 3 Amplitude values of axial and sagittal measurements, ICCs, and Bland-Altman coefficients in each cervical segment in all measurements

		Axial		Sagittal		Difference Axial – Sagittal		Coefficient of repeatability		Intraclass correlation coefficients			
Segment	*N*	Mean	SD	Mean	SD	Mean	SD	1.96 × SD	*p*	ICC	CI_{min}	CI_{max}	*p*
C2	62	0.51	0.28	0.48	0.25	0.02	0.12	0.23	.186	.902	.842	.940	<.001
C3	43	0.83	0.56	0.76	0.55	0.07	0.19	0.37	.001	.934	.871	.966	<.001
C4	51	0.83	0.48	0.94	0.53	−0.12	0.30	0.58	.008	.810	.669	.892	<.001
C5	54	1.05	0.54	1.04	0.53	0.01	0.19	0.36	.676	.940	.899	.965	<.001
C6	41	0.89	0.46	0.88	0.41	0.02	0.22	0.43	.600	.876	.779	.932	<.001

Note: The motion amplitude values (all measurements) are reported per cervical segment for axial and sagittal measurements. Additionally, the difference of axial minus sagittal values for each cervical segment is shown. The amplitude difference between axial and sagittal measurements was significantly different from 0 at segment C3 and C4. Intraclass correlation coefficients (ICCs; two-way mixed model, single measures, absolute agreement) with its 95% confidence interval (CI) are presented for each cervical segment.
Abbreviations: *N*, number of measurements; SD, standard deviation.

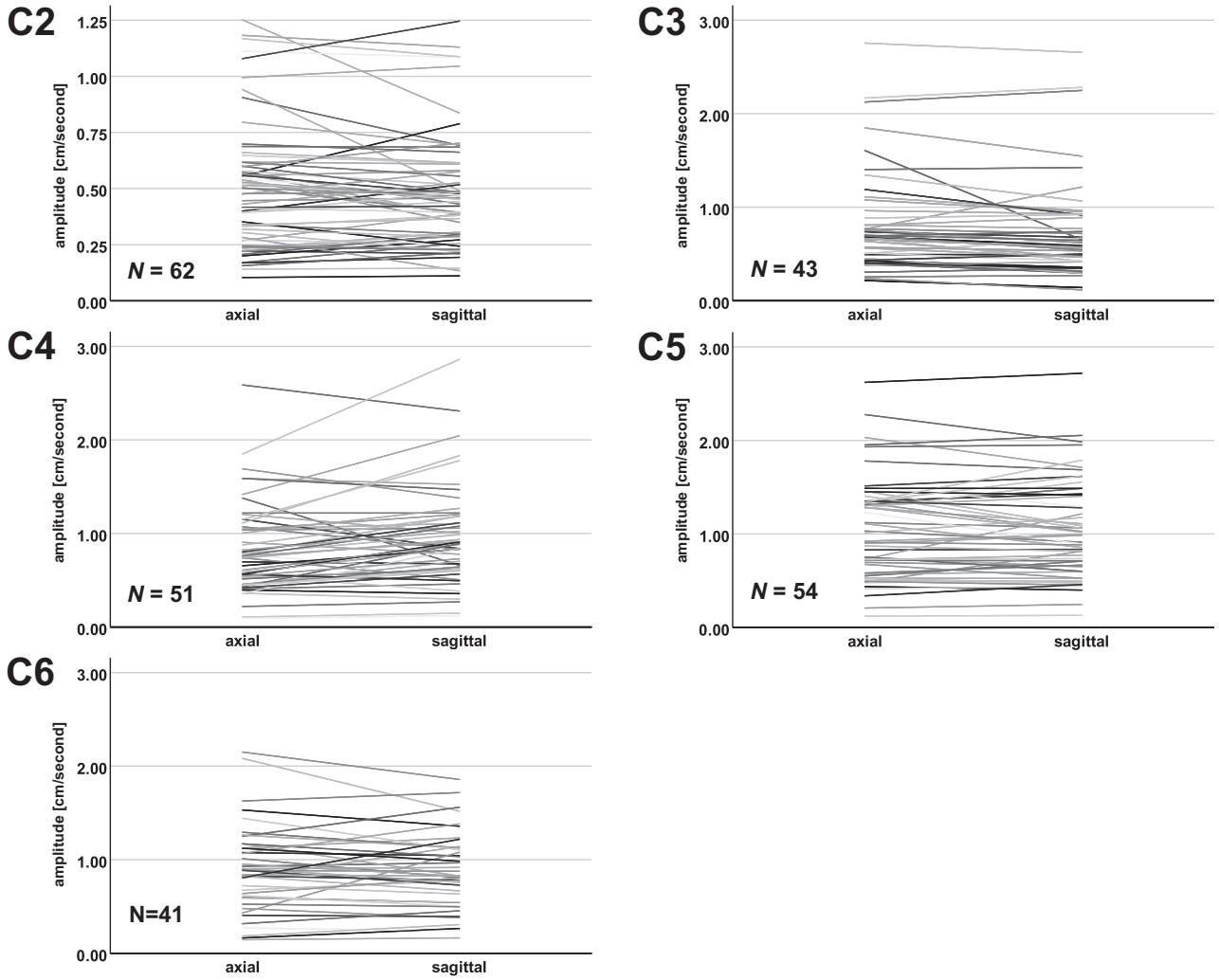

FIGURE 3 Individual segmental amplitude values in axial and sagittal phase contrast measurements. Individual segmental amplitude values for all measurements (venc 2 and 3 cm/second; stenotic and nonstenotic segments) are shown for each cervical segment. The individual axial and sagittal values are interconnected (lines) to illustrate the deviation between axial and sagittal measurements. *N*, number of measurements.

TABLE 4 Amplitude values of axial and sagittal measurements, ICCs, and Bland-Altman coefficients in each cervical segment in subgroups with different venc

Velocity encoding 2 cm/second													
		Axial		Sagittal		Bland-Altman coefficients				Intraclass correlation coefficients			
Segment	*N*	Mean	SD	Mean	SD	Mean	SD	1.96 × SD	*p*	ICC	CI_{min}	CI_{max}	*p*
C2	28	0.54	0.33	0.50	0.27	0.04	0.14	0.28	.362	.882	.762	.943	<.001
C3	10	0.97	0.64	0.88	0.62	0.10	0.36	0.70	.285	.843	.509	.958	.001
C4	19	1.05	0.59	0.96	0.58	0.09	0.26	0.52	.165	.894	.749	.958	<.001
C5	22	1.05	0.53	1.03	0.49	0.02	0.21	0.42	.638	.915	.808	.964	<.001
C6	10	1.00	0.25	0.96	0.24	0.04	0.19	0.36	.559	.732	.235	.926	.006
Velocity encoding 3 cm/second													
		Axial		Sagittal		Bland-Altman coefficients				Intraclass correlation coefficients			
Segment	*N*	Mean	SD	Mean	SD	Mean	SD	1.96 × SD	*p*	ICC	CI_{min}	CI_{max}	*p*
C2	34	0.47	0.22	0.46	0.24	0.01	0.09	0.17	.358	.931	.867	.965	<.001
C3	33	0.79	0.53	0.72	0.53	0.07	0.11	0.21	.001	.973	.914	.989	<.001
C4	32	0.70	0.34	0.93	0.51	−0.24	0.25	0.48	<.001	.734	.167	.899	<.001
C5	32	1.05	0.55	1.04	0.56	0.00	0.17	0.33	.921	.956	.912	.978	<.001
C6	31	0.86	0.51	0.85	0.45	0.01	0.23	0.45	.767	.887	.780	.944	<.001

Note: The motion amplitude values for the subgroups with venc 2 cm/second (upper table) and venc 3 cm/second (lower table) measurements are reported per cervical segment for axial and sagittal measurements. The amplitude difference of axial minus sagittal measurements was significantly different from 0 at segment C3 and C4 in the venc 3 cm/second subgroup. Intraclass correlation coefficients (ICCs; two-way mixed model, single measures, absolute agreement) with its 95% confidence interval (CI) are presented for each cervical segment.
Abbreviations: *N*, number of measurements; SD, standard deviation.

TABLE 5 Amplitude values of axial and sagittal measurements, ICCs, and Bland-Altman coefficients in each cervical segment in stenotic and nonstenotic segments

Nonstenotic segments													
		Axial		Sagittal		Bland-Altman coefficients				Intraclass correlation coefficients			
Segment	*N*	Mean	SD	Mean	SD	Mean	SD	1.96 × SD	*p*	ICC	CI_{min}	CI_{max}	*p*
C2	62	0.51	0.28	0.48	0.25	0.02	0.12	0.23	.186	.902	.842	.940	<.001
C3	24	0.63	0.24	0.58	0.23	0.06	0.10	0.19	.010	.896	.719	.958	<.001
C4	22	0.69	0.34	0.83	0.40	−0.14	0.27	0.53	.004	.687	.353	.861	<.001
C5	7	0.80	0.48	0.82	0.43	−0.02	0.07	0.13	.378	.990	.948	.998	<.001
C6	21	0.74	0.41	0.76	0.40	−0.02	0.20	0.39	.903	.883	.734	.951	<.001
Stenotic segments													
		Axial		Sagittal		Bland-Altman coefficients				Intraclass correlation coefficients			
Segment	*N*	Mean	SD	Mean	SD	Mean	SD	1.96 × SD	*p*	ICC	CI_{min}	CI_{max}	*p*
C2	0	na	Na	na	na	na	na	na	na	na	na	na	na
C3	19	1.09	0.72	0.99	0.73	0.10	0.27	0.52	.049	.928	.822	.972	<.001
C4	29	0.94	0.54	1.03	0.61	−0.09	0.31	0.62	.115	.842	.691	.923	<.001
C5	47	1.08	0.54	1.07	0.54	0.02	0.20	0.39	.587	.934	.884	.962	<.001
C6	20	1.06	0.47	1.00	0.39	0.06	0.23	0.46	.277	.849	.663	.937	<.001

Note: The motion amplitude values in subgroups with measurements in nonstenotic (upper table) and stenotic (lower table) segments are reported per cervical segment for axial and sagittal measurements. The amplitude difference between axial minus sagittal measurements was significantly different from 0 at segment C3 and C4 in nonstenotic segments and at segment C3 in stenotic segments. Intraclass correlation coefficients (ICCs; two-way mixed model, single measures, absolute agreement) with its 95% confidence interval (CI) are presented for each cervical segment.
Abbreviations: *N*, number of measurements; SD = standard deviation.

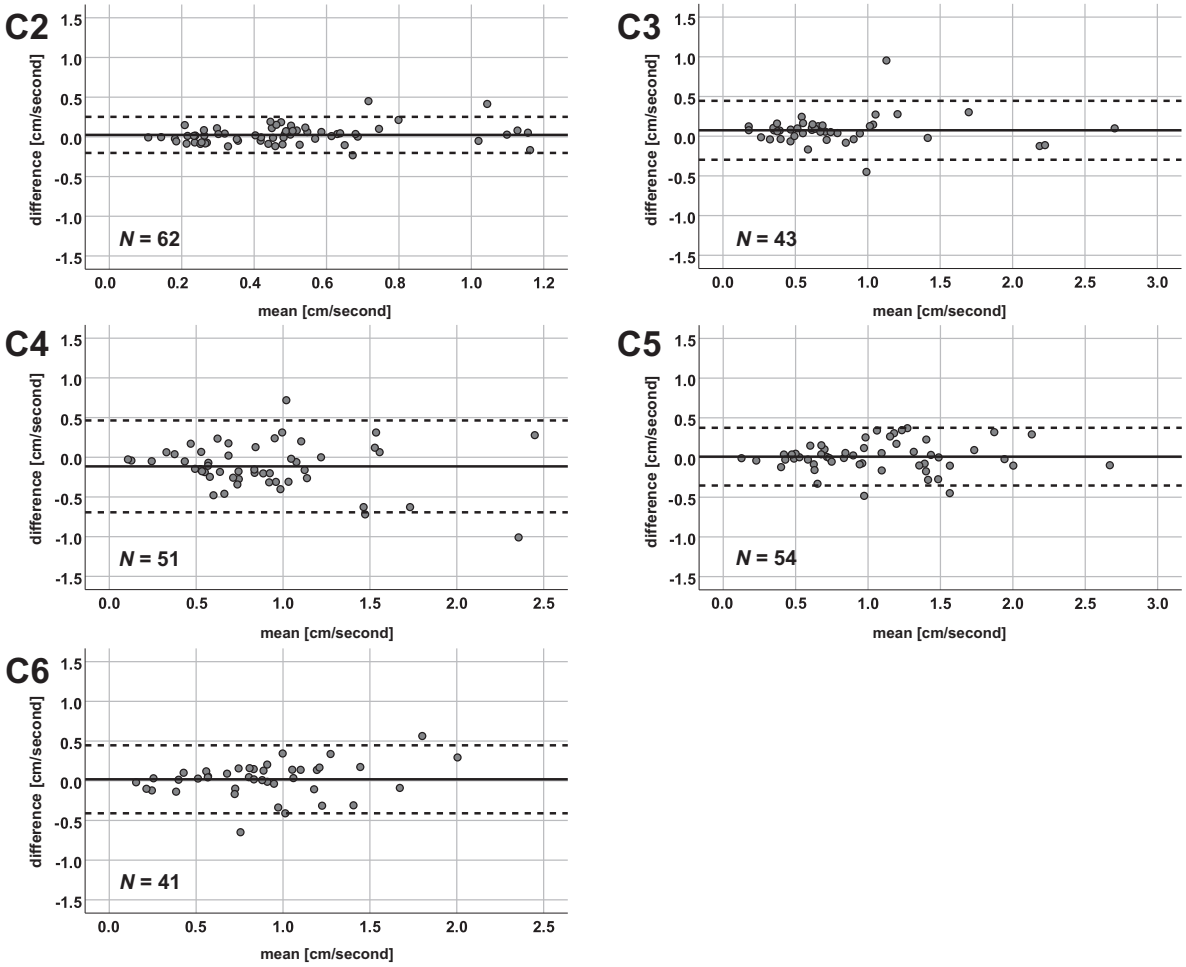

FIGURE 4 Bland-Altman plots for all measurements. The mean of the amplitudes (*x*-axis) and the differences of the axial minus sagittal amplitude values (*y*-axis) are plotted in each cervical segment. The solid horizontal line represents the mean of all measurement values, while the pointed lines represent the limits of agreement (1.96 × standard deviation). *N*, number of measurements.

Agreement of axial and sagittal measurements

Over all measurements (venc 2 and 3 cm/second; stenotic and non-stenotic segments), ICCs of axial and sagittal amplitude values showed good to excellent values in all segments (.810-.940; $p < .001$; Table 3). The Bland-Altmann readouts, that is, the measurement bias and limits of agreement, of the amplitude values in each cervical segment can be found in Table 3. The coefficients of repeatability (±1.96 SD of the mean difference between tests) ranged from 0.23 cm/second at segment C2 to 0.58 cm/second at C4. A summary of comparability analyses, that is, ICCs and Bland–Altman analysis, can be found in Table 3 and Figure 4.

In a subgroup analysis with regard to the different venc used in measurements, the ICCs ranged from .732 to .915 in measurements with venc 2 cm/second and from .734 to .973 in measurements with venc 3 cm/second (Table 4). The coefficients of repeatability in venc 2 cm/second measurements ranged from 0.28 cm/second at segment C2 to 0.70 cm/second at C3 (Table 4; Figure 5). In venc 3 cm/second measurements, it ranged from 0.17 cm/second at segment C2 to 0.48 cm/second at C4 (Table 4; Figure 5).

In measurements in nonstenotic segments, ICCs ranged from .687 to 0.990, and in stenotic segments from .842 to .934 (Table 5). The coefficients of repeatability in measurements in nonstenotic segments ranged from 0.13 cm/second at segment C5 to 0.53 cm/second at C4 (Table 5; Figure 6). In stenotic segments, it ranged from 0.39 cm/second at segment C5 to 0.62 cm/second at C4 (Table 5; Figure 6).

Amplitude differences with regard to the amplitude mean

A correlation between the segmental amplitude mean values and the differences of the amplitude values was found at C2 ($r = .256$; $p = .045$) and a trend for a correlation at segment C6 ($r = .284$; $p = .072$).

DISCUSSION

This study demonstrates a good comparability and agreement between axial and sagittal spinal cord motion PC-MRI in DCM patients. A

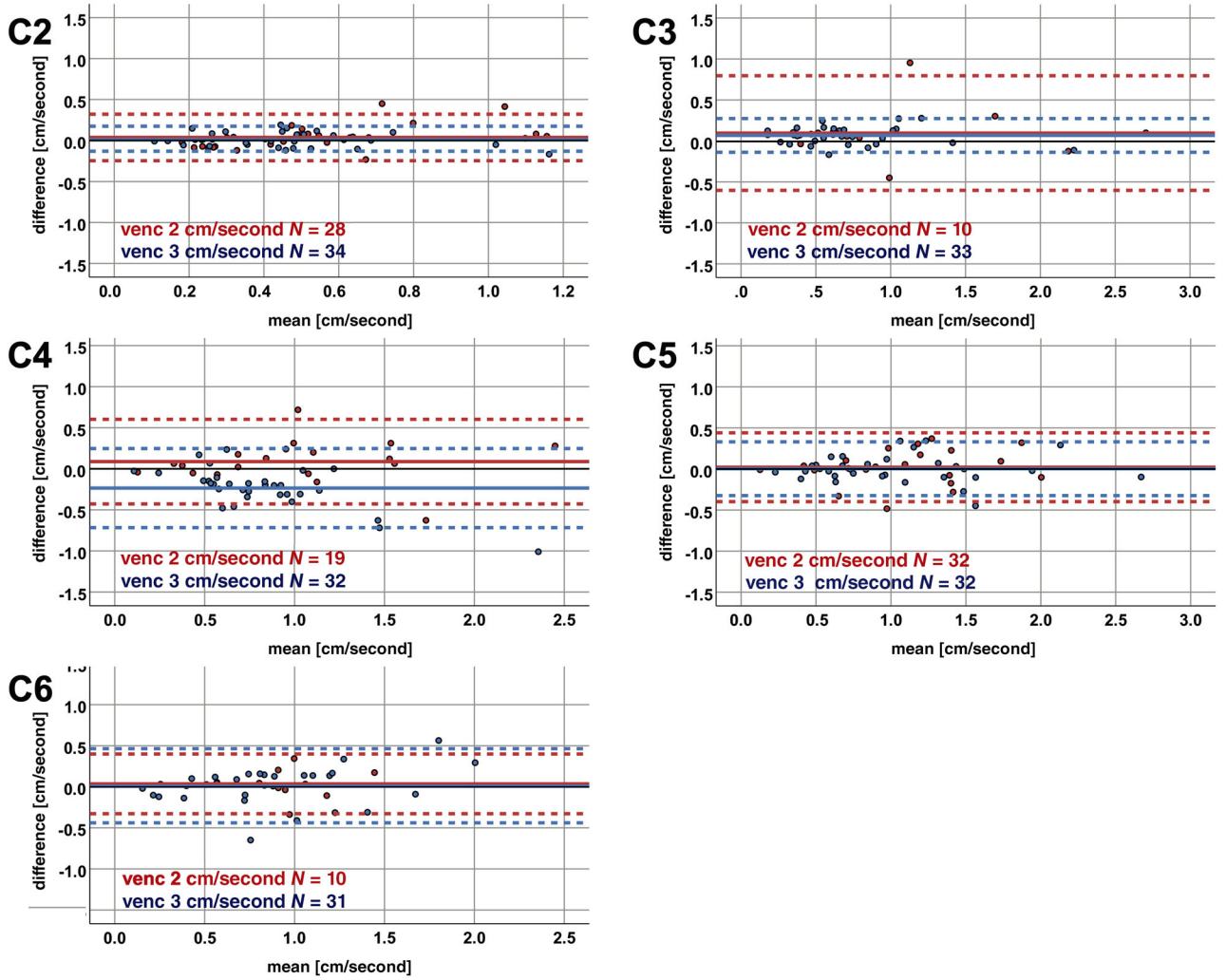

FIGURE 5 Bland-Altman plots for subgroups with velocity encoding of 2 versus 3 cm/second measurements. The mean of the amplitudes (*x*-axis) and the differences of the axial minus sagittal amplitude values (*y*-axis) are plotted in each cervical segment for measurements with velocity encoding (venc) of 2 cm/second (red color) versus venc 3 cm/second (blue color). The solid horizontal line represents the mean of all measurement values, while the pointed lines represent the limits of agreement (1.96 × standard deviation). The black solid horizontal line illustrates the 0 value reference for amplitude differences. *N*, number of measurements.

possible measurement error in sagittal PC-MRI through the spinal cord misalignment to the vertical reference line within the field of view appears to be negligible. However, a potential future clinical application would greatly benefit from a standardized MRI protocol and postprocessing pipeline, thus improving comparability of findings across different clinical centers.

Different techniques and numerous readouts measuring spinal cord motion reported in previous studies challenge the comparability between sites.[9–19,27–30] In our study, we decided to analyze the agreement of the motion amplitude between axial and sagittal measurements as an easy-to-collect readout with no need for a phase drift correction. Varying phase drift was reported across different scanners[31] and also over time in the same scanner,[32] potentially limiting the use of readouts with need for a phase drift correction like the area under the curve of the motion signal. To our knowledge, reproducibility of phase contrast measurements across different scanners was rarely analyzed,[33] where a substantial agreement but also a significant bias could be observed across different readouts of pulmonary blood flow measurements. Hence, the agreement for different spinal cord motion readouts has to be further evaluated across scanners. Importantly, the PC-MRI postprocessing for velocity calculations should be automated as far as possible, but also easy to be transferred and introduced across different clinical centers. Wolf et al. reported an evaluation technique using a 3-dimensional hierarchical deep convolutional neural network (CNN) for anatomical segmentation and spinal cord motion measurements.[16,17] This approach appears promising, as motion evaluation could be conducted automatically after appropriate training of the CNN. However, it may be challenging to widely transfer this technique to other centers in order to foster clinical application. Our group reported a manual method, using free available DICOM tools and manual calculation of velocity values.[9,11] This approach could be easily introduced at other centers, but remains

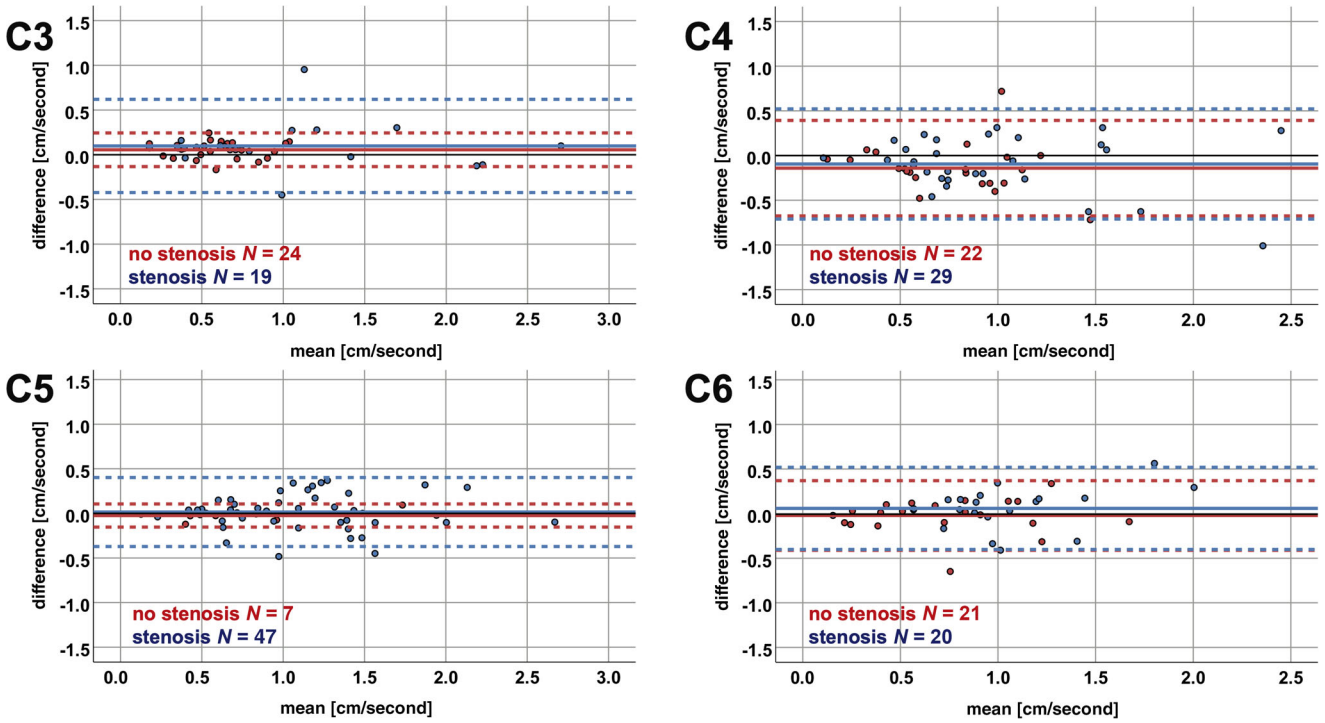

FIGURE 6 Bland-Altman plots for subgroups with measurements in nonstenotic versus stenotic segments. The mean of the amplitudes (*x*-axis) and the differences of the axial minus sagittal amplitude values (*y*-axis) are plotted in each cervical segment for measurements in nonstenotic segments (red color) and in stenotic segments (blue color). The solid horizontal lines represent the mean of all measurement values, while the pointed lines represent the limits of agreement (1.96 × standard deviation). The black solid horizontal line illustrates the 0 value reference for amplitude differences. *N*, number of measurements.

more time consuming and lacks further automatization. Reliability between different evaluation techniques (ie, automated vs. manual calculation) is not known. To further promote the implementation of spinal cord motion PC-MRI measurements within the clinical setting, comparison of different postprocessing techniques (ie, CNN vs. manual evaluation) between sites is mandatory. Furthermore, a proper venc in PC-MRI is important for spinal cord motion measurements, adapted as far as possible to the expected velocities.[34,35] While improper low venc causes aliasing artifacts, noise in velocity images increases with higher venc, probably leading to measurement errors.[36] In subgroup analyses with regard to different venc used in our measurements, a significant difference between axial and sagittal amplitude values could only be found at C3 and most obvious at C4 in venc 3 cm/second measurements and amplitude differences were higher in venc 3 cm/second compared to venc 2 cm/second measurements at C4. An increasing measurements error with higher velocity encoding was previously reported,[36] while this was relevant with an extensive higher venc only (ie, a deviation of more than 10% if venc increases by more than three times the velocity in the vessel). However, the magnitude of differences was low and aliasing artifacts could be observed in 5.6% of patients using a velocity encoding of 2 cm/second. In principle, aliasing artifacts within PC-MRI measurements could be corrected,[37] but this leads to more complicated and time-consuming postprocessing of the measurements. The question now turns to, whether it is advisable to choose a venc of 3 cm/second or a venc of 2 cm/second for spinal cord motion measurements. Considering the pros and cons, we recommend a velocity encoding of 3 cm/second for future measurements, where no further aliasing was noticed and the magnitude of differences observed appears to be acceptable for clinical use. However, venc may be further adjusted to an optimal value (eg, 2.5 cm/second) within establishment of a "gold standard" protocol for clinical implementation.

Previous studies reported excellent interrater and test-retest reliability of spinal cord motion measurements with axial and sagittal PC-MRI.[9,11,15,17] In addition, in our study we demonstrate a good to excellent[26] comparability and agreement of these two different PC-MRI measurement techniques (ie, axial and sagittal phase contrast imaging) of spinal cord motion in DCM patients. We hypothesized that a difference of velocity values in sagittal measurements compared to axial values might be mostly attributed to a systematic measurement error due to the misalignment of the spinal cord within the field of view. Significant differences between axial and sagittal amplitude values could only be found at C3 and C4, but not in segments C5 and C6 with higher spinal cord misalignment. Additionally, no correlation between the misalignment angle and the amplitude differences could be found, underlining the weak effect of this potential confounder. Thus, effect size of a systematic measurement error due to spinal cord misalignment within the field of view is supposed to be weak as values of sagittal measurements showed a good agreement to axial data without the need for a correction. The reason for less agreement between axial and sagittal amplitude values in segments C3 and C4

compared to other segments remains unexplained. With regard to the segmental anatomic conditions (ie, measurements in stenotic vs. nonstenotic segments), subgroup analysis showed a good to excellent comparability between axial and sagittal values in both subgroups. In previous reports, reliability of spinal cord motion measurements was not reported for stenotic and nonstenotic segments separately. Interestingly, measures of reliability in our population showed comparable to even better values of reliability (ie, higher ICC values) in stenotic segments and no disagreement of differences could be found between the subgroups with measurements in stenotic and nonstenotic segments. While the spinal cord is subject not only to a craniocaudal oscillation, but also to anterior-posterior and right-left motion,[38] measurements in stenotic segments may be more reliable due to narrowed anatomic conditions. Restricted anterior-posterior motion may limit potential partial volume effects between the spinal cord and CSF within the cardiac cycle reducing measurements errors. A weak correlation between the amplitude difference and the magnitude of the amplitude mean could be found at segment C2 only. While overall the magnitude of differences between axial and sagittal motion values appears acceptable for future clinical application, in a few measurements relevant differences could be observed, underlining the importance of a standardized measurement protocol to further improve comparability. In summary, phase contrast measurements of spinal cord motion have potential to be applied in the clinical settings, but pros and cons of different evaluation techniques have to be considered.

Sagittal PC-MRI can assess the entire cervical spine in one PC-MRI measurement. A potential systematic measurement error in sagittal PC-MRI through the spinal cord misalignment within the field of view (Figure 1) could be shown to be negligible. In contrast, axial measurements might be more precise, accounting for the spinal cord misalignment by adapting the measurement slice perpendicular to the spinal cord (Figure 1A), but are more time consuming, as each cervical segment has to be analyzed separately (ie, causing longer MRI measurement time, difficult to implement in clinical protocols). Sagittal phase contrast measurements appear as a good compromise between accuracy (good agreement to axial values; good interrater and test-retest reliability[17]; no need for a correction for the spinal cord misalignment) and feasibility (ie, shorter measurement time compared to separate axial measurements in each cervical segment) within the clinical setting.

This study has few limitations. As no analysis was possible at segment C7, where the maximum spinal cord misalignment to the vertical reference line was observed, a relevant systematic measurement error in segments with higher grade of spinal cord misalignment could not be excluded. However, spinal canal stenosis in these segments is rare and measurements in segment C6 (also considerable spinal cord misalignment) showed a good agreement. Another limitation of our study is based on the use of only one MRI scanner. Scanners from different MRI vendors may influence comparability across measurements. Additionally, further insights of reliability between different PC-MRI protocols and postprocessing techniques across centers are required to define a "gold standard" and to foster its clinical application in the diagnostic workup of DCM.

In conclusion, the confident assessment of spinal cord damage in DCM patients remains an unmet clinical need. There is evidence to support the use of spinal cord motion surrogate parameters in order to determine the degree of dynamic mechanical stress precipitating spinal cord damage. To this end, axial and sagittal PC-MRI are both accurate and sensitive in detecting pathologic cord motion. Therefore, such measures could identify high-risk patients and improve clinical decision-making (eg, timing of decompressive surgery).

ACKNOWLEDGEMENTS AND DISCLOSURES

We would like to thank all patients for participation in this study. We thank Regula Schuepbach and Nathalie Kuehne for the excellent organization of the examinations and the management of the RedCap database. We also would like to thank the MRI team, that is, Natalie Hinterholzer, Alexandra Conte, and Zoe Volkart for conduction of the MRI measurements. Imaging was partly performed with support of the Swiss Center for Musculoskeletal Imaging, SCMI, Balgrist Campus AG, Zurich. Open access funding provided by Universitat Zurich.

All authors do not disclose commercial considerations in the past 2 years, such as equity interests, patent rights, or corporate affiliations including director roles, stock ownership, consultancy, speaking fees, and research support, for any product or process relevant to the submission. Balgrist University Hospital and Balgrist Campus have an academic research agreement with Siemens Healthineers.

ORCID

Markus Hupp https://orcid.org/0000-0003-0845-2514

REFERENCES

1. Zipser CM, Margetis K, Pedro KM, et al. Increasing awareness of degenerative cervical myelopathy: a preventative cause of non-traumatic spinal cord injury. Spinal Cord. 2021;59:1216-8.
2. Kalsi-Ryan S, Karadimas SK, Fehlings MG. Cervical spondylotic myelopathy: the clinical phenomenon and the current pathobiology of an increasingly prevalent and devastating disorder. Neuroscientist. 2013;19:409-21.
3. Fehlings MG, Kwon BK, Tetreault LA. Guidelines for the management of degenerative cervical myelopathy and spinal cord injury: an introduction to a focus issue. Global Spine J. 2017;7:6S-7S.
4. Tetreault L, Nouri A, Kopjar B, et al. The minimum clinically important difference of the modified Japanese Orthopaedic Association scale in patients with degenerative cervical myelopathy. Spine. 2015;40:1653-9.
5. Karadimas SK, Moon ES, Yu WR, et al. A novel experimental model of cervical spondylotic myelopathy (CSM) to facilitate translational research. Neurobiol Dis. 2013;54:43-58.
6. Karadimas SK, Gatzounis G, Fehlings MG. Pathobiology of cervical spondylotic myelopathy. Eur Spine J. 2015;24:132-8.
7. Karadimas SK, Klironomos G, Papachristou DJ, et al. Immunohistochemical profile of NF-kappaB/p50, NF-kappaB/p65, MMP-9, MMP-2, and u-PA in experimental cervical spondylotic myelopathy. Spine. 2013;38:4-10.
8. Beattie MS, Manley GT. Tight squeeze, slow burn: inflammation and the aetiology of cervical myelopathy. Brain. 2011;134:1259-61.
9. Hupp M, Vallotton K, Brockmann C, et al. Segmental differences of cervical spinal cord motion: advancing from confounders to a diagnostic tool. Sci Rep. 2019;9:7415.

10. Mikulis DJ, Wood ML, Zerdoner OA, et al. Oscillatory motion of the normal cervical spinal cord. Radiology. 1994;192:117-21.
11. Hupp M, Pfender N, Vallotton K, et al. The restless spinal cord in degenerative cervical myelopathy. AJNR Am J Neuroradiol. 2021;42:597-609.
12. Chang HS, Nejo T, Yoshida S, et al. Increased flow signal in compressed segments of the spinal cord in patients with cervical spondylotic myelopathy. Spine. 2014;39:2136-42.
13. Tanaka H, Sakurai K, Iwasaki M, et al. Craniocaudal motion velocity in the cervical spinal cord in degenerative disease as shown by MR imaging. Acta Radiol. 1997;38:803-9.
14. Vavasour IM, Meyers SM, Macmillan EL, et al. Increased spinal cord movements in cervical spondylotic myelopathy. Spine J. 2014;14:2344-54.
15. Wolf K, Hupp M, Friedl S, et al. In cervical spondylotic myelopathy spinal cord motion is focally increased at the level of stenosis: a controlled cross-sectional study. Spinal Cord. 2018;56:769-76.
16. Wolf K, Reisert M, Beltran SF, et al. Spinal cord motion in degenerative cervical myelopathy: the level of the stenotic segment and gender cause altered pathodynamics. J Clin Med. 2021;10:3788.
17. Wolf K, Reisert M, Beltran SF, et al. Focal cervical spinal stenosis causes mechanical strain on the entire cervical spinal cord tissue - a prospective controlled, matched-pair analysis based on phase-contrast MRI. Neuroimage Clin. 2021;30:102580.
18. Tanaka H, Sakurai K, Kashiwagi N, et al. Transition of the craniocaudal velocity of the spinal cord: from cervical segment to lumbar enlargement. Invest Radiol. 1998;33:141-5.
19. Levy LM, Di Chiro G, Mccullough DC, et al. Fixed spinal cord: diagnosis with MR imaging. Radiology. 1988;169:773-8.
20. Kato S, Oshima Y, Oka H, et al. Comparison of the Japanese Orthopaedic association (JOA) score and modified JOA (mJOA) score for the assessment of cervical myelopathy: a multicenter observational study. PLoS ONE. 2015;10:e0123022.
21. Rupp R, Biering-Sorensen F, Burns SP, et al. International standards for neurological classification of spinal cord injury: revised 2019. Top Spinal Cord Inj Rehabil. 2021;27:1-22.
22. Velstra I-M, Fellinghauer C, Abel R, et al. The graded and redefined assessment of strength, sensibility, and prehension version 2 provides interval measure properties. J Neurotrauma. 2018;35:854-63.
23. Fehlings MG, Badhiwala JH, Ahn H, et al. Safety and efficacy of riluzole in patients undergoing decompressive surgery for degenerative cervical myelopathy (CSM-Protect): a multicentre, double-blind, placebo-controlled, randomised, phase 3 trial. Lancet Neurol. 2021;20:98-106.
24. Harris PA, Taylor R, Thielke R, et al. Research electronic data capture (REDCap)–a metadata-driven methodology and workflow process for providing translational research informatics support. J Biomed Inform. 2009;42:377-81.
25. Martin Bland J, Altman D. Statistical methods for assessing agreement between two methods of clinical measurement. Lancet. 1986;1:307-10.
26. Koo TK, Li MY. A guideline of selecting and reporting intraclass correlation coefficients for reliability research. J Chiropr Med. 2016;15:155-63.
27. Winklhofer S, Schoth F, Stolzmann P, et al. Spinal cord motion: influence of respiration and cardiac cycle. Rofo. 2014;186:1016-21.
28. Figley CR, Stroman PW. Investigation of human cervical and upper thoracic spinal cord motion: implications for imaging spinal cord structure and function. Magn Reson Med. 2007;58:185-9.
29. Enzmann DR, Pelc NJ. Brain motion: measurement with phase-contrast MR imaging. Radiology. 1992;185:653-60.
30. Matsuzaki H, Wakabayashi K, Ishihara K, et al. The origin and significance of spinal cord pulsation. Spinal Cord. 1996;34:422-6.
31. Minderhoud SCS, Van Der Velde N, Wentzel JJ, et al. The clinical impact of phase offset errors and different correction methods in cardiovascular magnetic resonance phase contrast imaging: a multi-scanner study. J Cardiovasc Magn Reson. 2020;22:68.
32. Gatehouse PD, Rolf MP, Bloch KM, et al. A multi-center inter-manufacturer study of the temporal stability of phase-contrast velocity mapping background offset errors. J Cardiovasc Magn Reson. 2012;14:72.
33. Iraha R, Tsuchiya N, Yamashiro T, et al. Reproducibility of pulmonary blood flow measurements by phase-contrast MRI using different 1.5 T MR scanners at two institutions. Acta Radiol Open. 2017;6:2058460116684370.
34. Korbecki A, Zimny A, Podgórski PA, et al. Imaging of cerebrospinal fluid flow: fundamentals, techniques, and clinical applications of phase-contrast magnetic resonance imaging. Pol J Radiol. 2019;84:240-50.
35. Villa G, Ringgaard S, Hermann I, et al. Phase-contrast magnetic resonance imaging to assess renal perfusion: a systematic review and statement paper. MAGMA 2020;33:3-21.
36. Lotz J, Meier C, Leppert A, et al. Cardiovascular flow measurement with phase-contrast MR imaging: basic facts and implementation. Radiographics. 2002;22:651-71.
37. Yang GZ, Burger P, Kilner PJ, et al. Dynamic range extension of cine velocity measurements using motion-registered spatiotemporal phase unwrapping. J Magn Reson Imaging. 1996;6:495-502.
38. Oztek MA, Mayr NA, Mossa-Basha M, et al. The dancing cord: inherent spinal cord motion and its effect on cord dose in spine stereotactic body radiation therapy. Neurosurgery. 2020;87:1157-66.

How to cite this article: Pfender N, Rosner J, Zipser CM, Friedl S, Vallotton K, Sutter R, et al. Comparison of axial and sagittal spinal cord motion measurements in degenerative cervical myelopathy. J Neuroimaging. 2022;1–13.
https://doi.org/10.1111/jon.13035